

Wake characteristics of two-dimensional perforated plates normal to an air-stream

By I. P. CASTRO

Department of Aeronautics, Imperial College, London, S.W. 7

(Received 14 August 1970)

The flow in the wakes behind two-dimensional perforated plates has been investigated in the Reynolds number range 2.5×10^4 to 9.0×10^4 .

Measurements of drag and shedding frequency were made and a pulsed hot-wire anemometer was used to measure the mean velocity and turbulent intensity variations in the highly turbulent regions immediately behind the plates.

The results indicate the existence of two distinct types of flows: one appropriate to high and the other to low values of plate porosity.

1. Introduction

There have been a number of attempts made, both in the past (Taylor 1944) and more recently (Valensi & Rebont 1969), to predict theoretically and measure experimentally the drag coefficient of two-dimensional perforated plates placed normal to an air-stream. The work presented here was originally intended as a continuation of the work described by Blockley (1968), who measured the resistance coefficients and the drag coefficients of such plates to compare with Taylor's theoretical work. It was felt that a more detailed investigation of the wake would not only be of interest in itself, but would also help to explain, and perhaps predict, the flow around, for instance, lattice-type structures or groups of buildings.

However, it became evident as the work continued that the results in some respects disagreed with the previous measurements of Blockley, and also with similar work by Valensi & Rebont (1969). On the other hand, there were striking similarities with the results presented by various authors, in particular Roshko (1954), Bearman (1965, 1966) and Wood (1964), who investigated the effect of various types of wake interference on a separated base flow. It is for this latter reason that it seems worth while to present this work.

2. Experimental arrangements

The main body of the work was done in the 3×2 ft. working section, low-speed, closed-return wind tunnel of the Aeronautics Department at Imperial College. A set of eleven perforated plates were made, details of which are shown in figure 1. By varying the hole diameter from plate to plate, a range of porosity β of 0.0–0.645 was obtained. The plates were supported normal to the free-stream direction across the 2 ft. length of the working section.

In general, the following tests were made on each plate: (i) measurement of the drag coefficient; (ii) measurement of the vortex shedding frequency; (iii) measurements of the mean u -component velocity and the turbulent intensity along a line normal to the plate centre-line and parallel to the tunnel axis.

A pulsed hot-wire anemometer of the sort described by Bradbury & Castro (1970) was used for the velocity and turbulent intensity measurements in regions where an ordinary hot wire would give misleading results, but otherwise completely standard equipment and techniques were used.

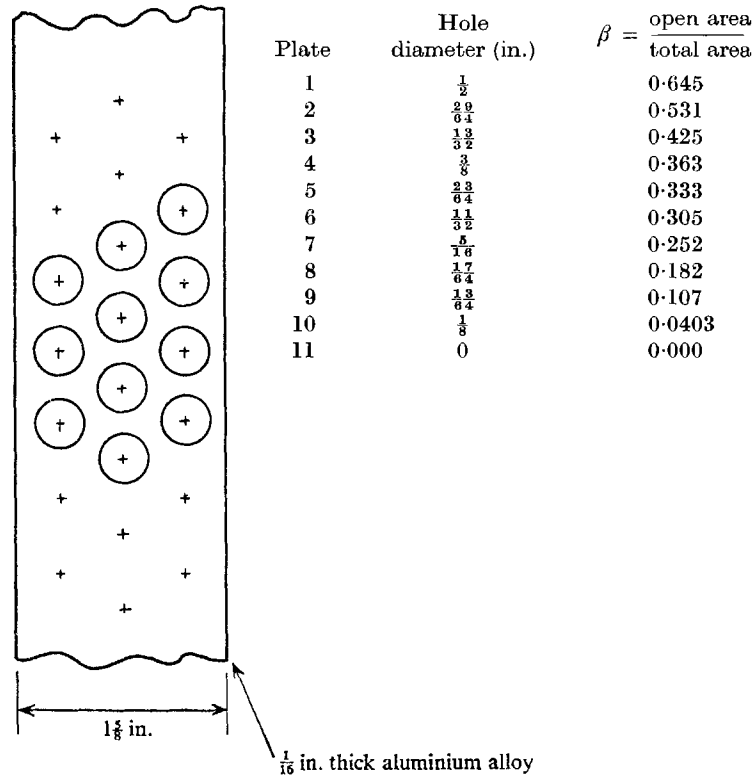


FIGURE 1. Details of perforated plates.

3. Results

Drag coefficient

The drag of each plate was measured by the wake traverse method. Betz (1925) has shown that the drag coefficient, defined in the usual way as

$$C_D = \text{drag force} / \frac{1}{2} \rho U_0^2 A,$$

where U_0 is the free-stream velocity and A is the plate area, is given by

$$C_D = (2/c) \int F dy + \text{terms involving the transverse mean velocities}, \quad (1)$$

where c is the plate chord width and F is given by

$$F = \frac{H_1 - H_2}{H_1 - p_1} - \left[\left(\frac{H_1 - p_2}{H_1 - p_1} \right)^{\frac{1}{2}} - \left(\frac{H_2 - p_2}{H_1 - p_1} \right)^{\frac{1}{2}} \right].$$

H and p are the total head and static pressures and suffices 1 and 2 refer to positions upstream and downstream respectively of the plate.

In a turbulent wake there will also be terms involving the fluctuating velocities. Any simple wake traverse method for determining the drag, particularly of a bluff body where there may be large transverse and fluctuating velocities, is subject to error as Maull & Bearman (1964) have pointed out. If the wake traverse is carried out near the body, the transverse and fluctuating velocity terms in equation (1) may well be significant. There will also be greater uncertainty in the measurement of static pressure, and to a lesser extent total head, than if the traverse is carried out far downstream. Consequently, to ensure that errors of this nature were as small as possible, the traverse for the unperforated plate was carried out at the far end of the working section. This corresponded to about 45 plate chord widths downstream, and the longitudinal turbulent intensity at this position was about 8% of the free-stream velocity. Since the object was to compare the drag of each plate, the traverses were all done at positions where the turbulent intensity was 8%, a technique suggested by Maull & Bearman (1964).

There was no particular reason for using Betz's formula rather than the more usual Jones one for the determination of the drag. Jones (1936) shows that if the static pressure at the traverse position is much lower than the lowest total pressure the two methods are identical, and in fact the difference between the two formulae was found to be less than 1% in the present experiment.

It became possible at a later date to measure the drag directly using a drag balance. The plates were supported in a 2 ft. octagonal tunnel on two stings about 9 in. apart, connected directly to a simple balance. This method of determining drag also presents difficulties, mainly in deducing suitable corrections for the end-effects. In this case the plates spanned the tunnel and passed through small slots in the side walls. The wall boundary layers would presumably cause an apparent decrease in the drag force from the two-dimensional case, but the tunnel working section was at sub-atmospheric static pressure, so that air flow through the slots in the side walls would also have some effect. A correction was made for the drag of the two supports but no corrections for end-effects have been applied.

Figure 2 shows a plot of the drag coefficient, C_D , obtained by the two methods, against $1/\beta^2$, which is used as an ordinate partly for clarity and partly for comparison with Blockley's results. $1/\beta^2$ is a relevant parameter in Taylor's theory. C_D has been corrected for blockage using Maskell's (1965) theory. The wake traverse results cannot be guaranteed to more than 5% or 6% on an absolute basis, but they were repeatable to within 3%. The balance measurements could also be in error by as much as 5%, but the two sets of results show at least qualitative agreement, and in fact nowhere differ by more than 7%. The few published values of the drag coefficient of a flat plate show variations of at

least 5%. Probably the most reliable result is that obtained from pressure distributions by Fage & Johanson (1927). They give a value of 2.13, which, as both Fail, Lawford & Eyre (1959) and Maskell (1965) show, reduces to 1.86 when blockage corrections are applied. This compares with the present results of 1.85 from the wake traverse and 1.89 for the balance measurement.

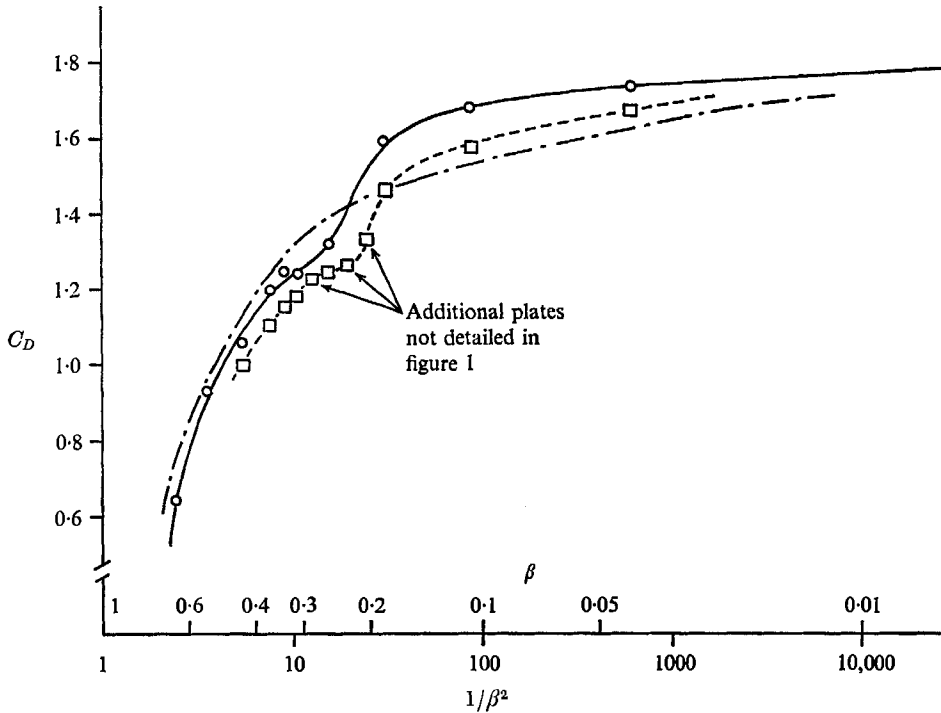


FIGURE 2. Drag coefficient vs. $1/\beta^2$. $Re = 9 \times 10^4$. ---, Blockley (1968); —○—, wake traverse method, $C_D = 1.85$ at $\beta = 0$; ---□---, drag balance method, $C_D = 1.89$ at $\beta = 0$.

At high values of β the results (figure 2) agree quite well with those of Blockley and indeed with the theoretical predictions of Taylor (which are only valid for C_D less than unity). However, at lower values of β (high $1/\beta^2$) agreement is not so good. This can be attributed in part to the fact that Blockley's perforated plates were considerably larger than the ones used in the present work, so that blockage corrections, which amounted to over 30% of the measured C_D in the worst case, were probably inadequate.

The main feature of this plot – and it is a phenomenon which neither Blockley's nor Valensi & Rebont's (1969) results indicate – is the distinct kink which occurs at a β of about 0.2. More recent work by Mitchell (1970) has shown that this kink is in fact more abrupt than figure 2 suggests.

Shedding frequency

The vortex shedding frequency was measured by placing a hot wire outside the wake to obtain a clear shedding signal. Figure 3 shows the Strouhal number, defined in the usual way as $S = fc/U_0$, where f is the shedding frequency and U_0

the corrected free-stream speed, plotted against $1/\beta^2$. As β increases there is a gradual increase in Strouhal number until, at $\beta = 0.2$, there is an abrupt reversal of slope. However, there is still a distinct peak in the spectrum, and only when β exceeded about 0.4 did this peak begin to spread over a range of values, and it was no longer possible to pinpoint any dominant frequency. Figure 3 therefore shows a band of possible values of S at these high values of porosity.

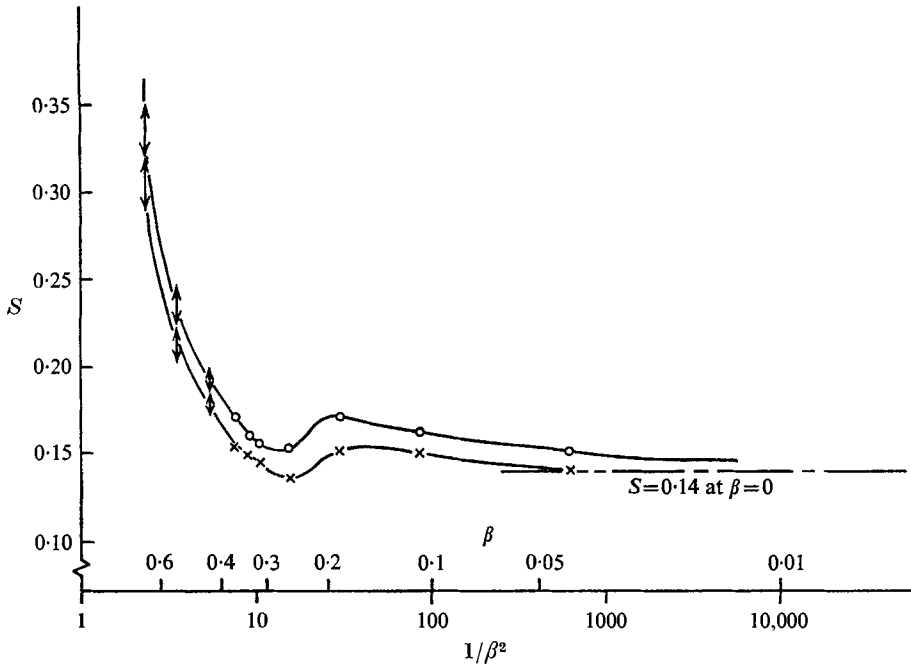


FIGURE 3. Strouhal number vs. $1/\beta^2$. —○—, $Re = 2.5 \times 10^4$;
—×—, $Re = 9.0 \times 10^4$; \updownarrow , band of S values.

The Strouhal number was measured over a range of Reynolds numbers, but only the two sets of results corresponding to the two limits of the range are shown. A typical variation of Strouhal number with Reynolds number is shown in figure 4, and this effect must be a consequence of the presence of the holes. It is not present for the non-perforated plate, and does not affect the general shape of the Strouhal number variation with β . Mitchell (1970) has also noticed a variation of drag coefficient with Reynolds number, which again is not present for the non-perforated plate and has no effect on the existence or position of the kink at a β of 0.2.

Longitudinal velocity and turbulent intensity

In order to obtain a simple picture of the flow field behind each plate, the u -component velocity and turbulent intensity were measured along a line parallel to the tunnel axis and normal to the centre-line of the plates. Standard commercial hot-wire apparatus was used where possible and the hot wire was set normal to the free-stream direction and traversed longitudinally along an axis of the central hole in each plate.

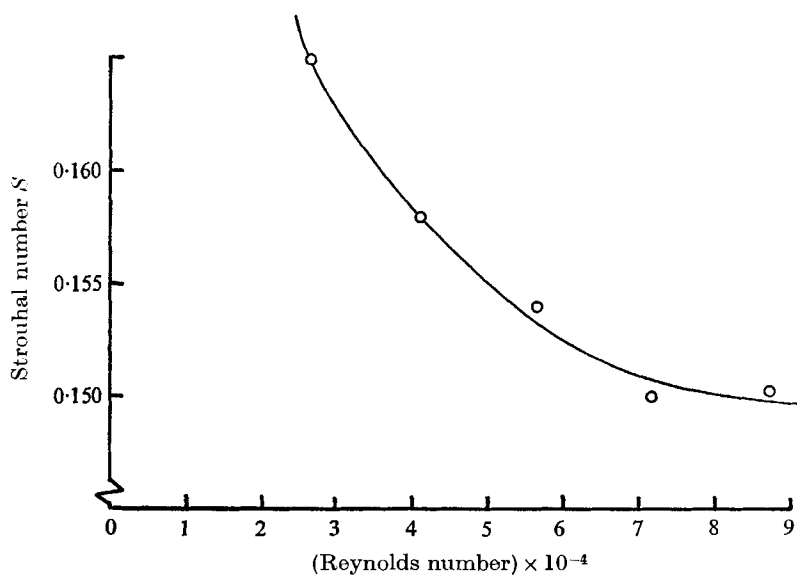


FIGURE 4. Typical variation of Strouhal number with Reynolds number, $\beta = 0.107$ (plate 9).

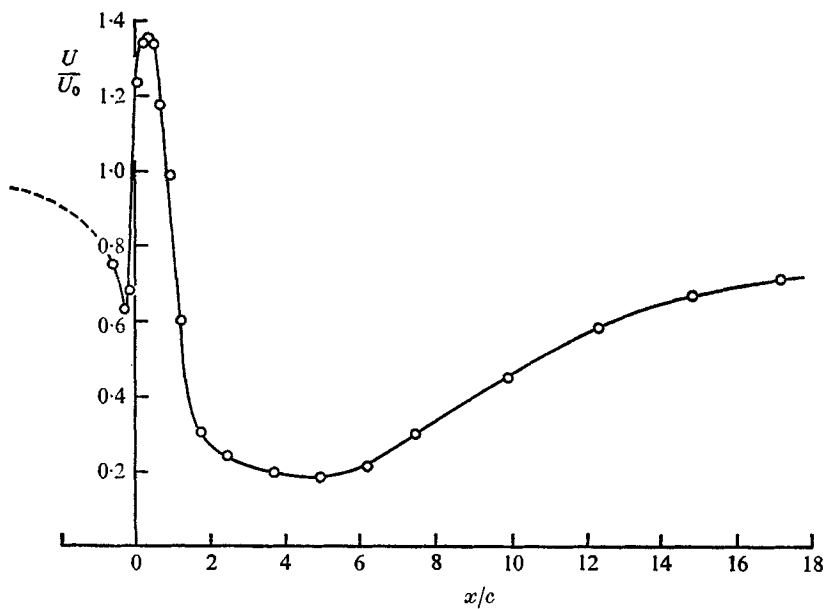


FIGURE 5. Typical variation of mean velocity behind a plate with high β . $\beta = 0.425$ (plate 3).

A typical non-dimensional plot of the mean velocity, U , against distance downstream, x , is shown in figure 5, for a plate with high porosity. The corresponding turbulent intensity, $\overline{u^2}$, is shown in figure 6. The initial large peak in intensity is presumably associated with the instability of the small jets of fluid coming through the plate. This is supported by the observation that most of the energy occurred at a particular, and quite a high, frequency which rose as the hole diameter was decreased. It is the flow through the holes themselves which presumably initiates the variations of drag and shedding frequency with Reynolds number, but it is a relatively unimportant region as far as understanding the general wake mechanism is concerned.

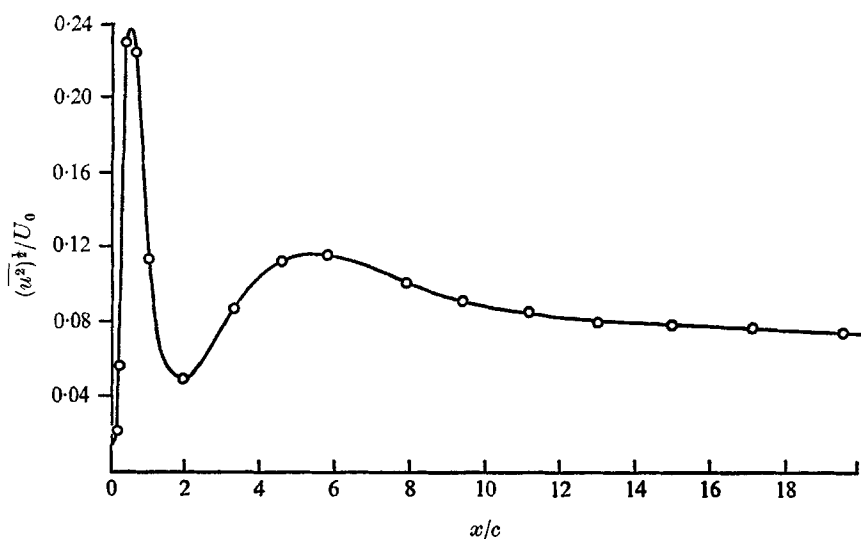


FIGURE 6. Typical variation of turbulent intensity behind a plate of high β .
 $\beta = 0.425$ (plate 3).

For cases of low porosity ($\beta < 0.3$), where the turbulent fluctuations in the near wake were much too high for hot-wire work, the mean velocity and turbulent intensity were measured using a pulsed hot-wire anemometer. This instrument, unlike an ordinary hot wire, is essentially linear and, more important, it has a well-defined yaw response and can measure velocities even in reversed-flow regions. When the present work was undertaken the instrument was still in a very early form, but has since been developed considerably and is fully described by Bradbury & Castro (1970).

A typical plot of the mean velocity variation obtained with a pulsed hot wire, behind a low-porosity plate, is shown in figure 7. It is clear that the reversed flow bubble which exists behind an ordinary flat plate has detached and moved downstream, so that there are two stagnation points, one at either end of the bubble. Figure 8 shows the corresponding turbulent intensity variation. The first main peak, just downstream of the bubble, corresponds to the position of vortex formation (Bearman 1965), but the meaning of the second peak is not clear. (The initial jet instability peak is of course still present.) It coincides with

a curious dip in the velocity variation of figure 7, and like the latter was present for all values of β up to about 0.2, although both gradually faded with increasing β . There may be some sort of standing wave pattern in the wake, but why and how this arises is difficult to explain.

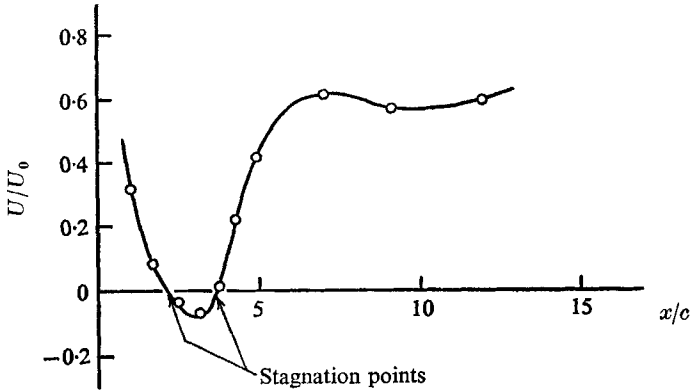


FIGURE 7. Typical plot of mean velocity variation at a low porosity.
 $\beta = 0.182$ (plate 8).

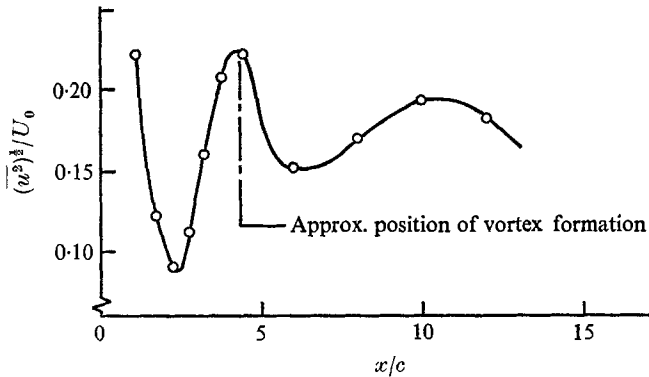


FIGURE 8. Typical plot of the turbulent intensity variation at a low porosity.
 $\beta = 0.182$ (plate 8).

Although velocity traverses were only made in the x direction, it was possible from the complete set of results to build up a reasonably clear picture of the flow pattern behind each plate. These are shown pictorially in figure 9 for the important cases. The flow is of course very unsteady, so that these sketches are only pictures of the 'average' state of the wake. The sketches are to scale in the x direction, and subsequent lateral velocity traverses done by Mitchell (1970) have shown that the bubble shapes depicted in figure 9 are about right.

4. Discussion

The mechanics of the separated base flow and vortex formation, although not fully understood, have been well documented in the past. In particular, some interesting work has been done on the effect of wake interference on these

processes, and the results already described seem to fall in line with these previous observations.

As is well known, a bluff body usually sheds two shear layers which are unstable and interact in the near wake, rolling up to form the vortex street. However, if the two separating shear layers are prevented from interacting in the usual way, the vortex formation may be delayed. Bearman (1966) and Wood (1964) have both shown that, if some bleed air is introduced into the wake of a blunt-based aerofoil, the vortex formation point moves downstream. There is a corresponding increase in Strouhal number and base pressure (and hence a lower drag). (A splitter plate has the same effect.) The two shear layers cannot now meet, due to the extra air injected between them, but they still interact to form a vortex street, although this is now weaker.

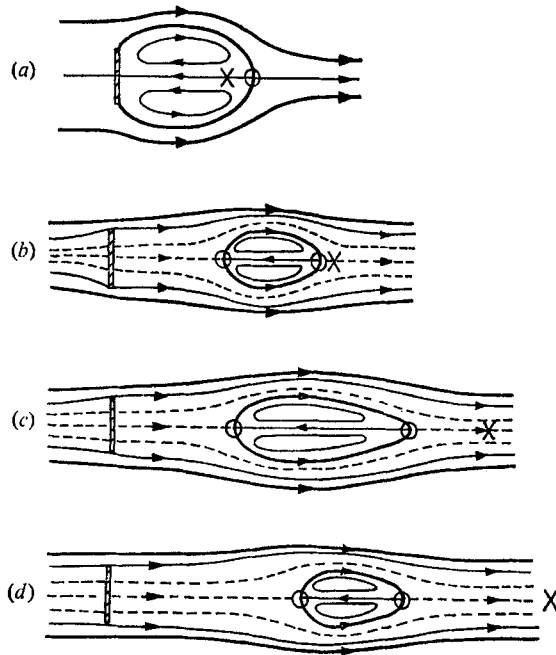


FIGURE 9. The effect of β on the near wake. \times , points of maximum turbulent intensity; ---, bleed air; \circ , stagnation points. (a) $\beta = 0$. (b) $\beta = 0.182$. (c) $\beta = 0.252$. (d) $\beta = 0.305$.

Figures 2 and 3 both show these initial trends. As the plate porosity increases, the shedding frequency rises and the drag drops. To conserve the mass balance across the wake there still has to be a reversed flow region, and this moves downstream with increasing β (figure 9(a), (b)). Figure 9 is very similar to the flow pattern suggested by Bearman (1966), although he was unable to show the existence of the bubble by direct measurement. The positions of maximum turbulent intensity (shown in figure 9) are plotted against β in figure 10, and it is clear that the vortex formation position also moves downstream.

However, this process does not continue. At a β of about 0.2 there are quite abrupt changes in all the parameters. Figure 2 shows a sudden drop in drag coefficient. A smooth continuation of the drag coefficient curve at high values of β into the low β range runs out somewhat lower than the curve which actually obtains at low values of β . Now the drag of a body shedding a vortex street is substantially higher than if the vortex street were not present, so figure 2 suggests that at a β of 0.2 the vortex street suddenly ceases to exist (rather than 'dying out' gradually). Figures 9 and 10 show that the peak in turbulent intensity moves off suddenly downstream at this value of β , and figure 3 shows that there is a corresponding drop in the Strouhal number. It seems that a critical point has been reached, at which there is just enough bleed air to prevent the shear layers from interacting at all to form a vortex street. If this is the case, one cannot really talk of a 'shedding frequency' or 'Strouhal number' in the usual sense beyond this critical value of β , but there is still a dominant frequency.

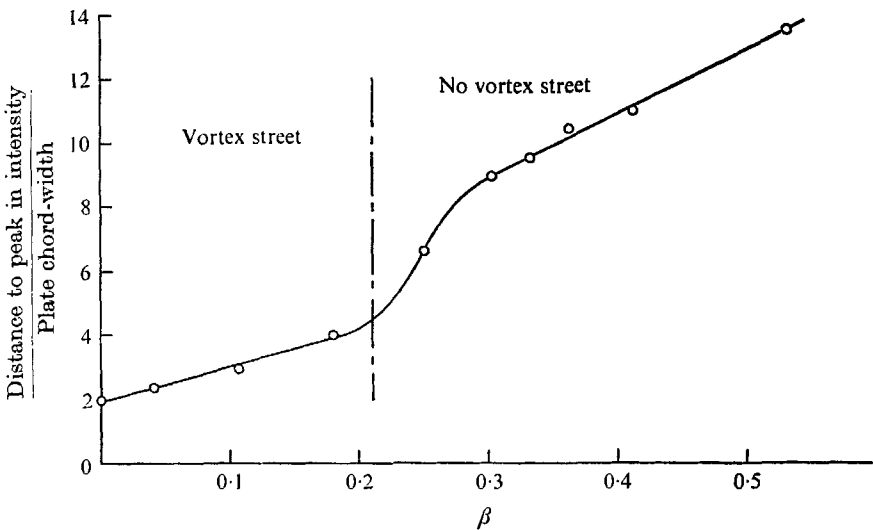


FIGURE 10. Variation of distance to peak in turbulent intensity with β .

This may be due to some sort of far wake instability. The flow round the plate itself is now essentially steady, but the two shear layers (with the bleed air in between) coalesce some way downstream, and the turbulent wake is unstable and starts to 'flap'. This would explain the continued periodic effect, and the fact that its onset is considerably further downstream.

It is interesting that for $\beta = 0.252$ and 0.305 a reversed flow bubble still exists. Evidently there is sufficient bleed air to prevent the vortex formation, but not enough to provide the entrainment needs of the shear layers, and it is only when this latter condition is fulfilled that the bubble disappears.

5. Conclusions

There are certainly two distinct régimes of flow. In one, appropriate to low values of porosity, the vortex street dominates the wake, although its strength gradually decreases as the vorticity in the shear layers decreases with the introduction of bleed air. The reversed flow region and the vortex formation region move downstream.

The nature of the flow at high porosities is open to suggestion, but it seems probable that the vortex street is not present, and the periodic effects are caused by a far wake instability, whilst there is no doubt that the transition between the two flow régimes is quite sudden.

The author wishes to acknowledge the helpful suggestions of Dr A. J. Taylor-Russell, who supervised the research. The author was in receipt of a Science Research Council grant.

REFERENCES

- BEARMAN, P. W. 1965 *J. Fluid Mech.* **21**, 241–255.
BEARMAN, P. W. 1966 *Agard C.P.* no. 4, 479–508.
BETZ, A. 1925 *Z. Flugtechn. Motor-Luftschiffahrt*, **16**, 42.
BLOCKLEY, R. H. 1968 M.Sc. thesis, University of London.
BRADBURY, L. J. S. & CASTRO, I. P. 1970 To be published.
PAGE, A. & JOHANSEN, F. C. 1927 *Aero. Res. Council. R. & M.* no. 1104.
FAIL, R., LAWFORD, J. A. & EYRE, R. C. W. 1959 *Aero. Res. Council. R. & M.* no. 3120.
JONES, B. M. 1936 *Aero. Res. Council. R. & M.* no. 1688.
MASKELL, E. C. 1965 *Aero. Res. Council. R. & M.* no. 3400.
MAULL, D. J. & BEARMAN, P. W. 1964 *J. Roy. Aero. Soc.* **68**, 843.
MITCHELL, J. 1970 M.Sc. thesis, University of London.
ROSHKO, A. 1954 *J. Fluid Mech.* **10**, 345–356.
TAYLOR, G. I. 1944 *Aero. Res. Council. R. & M.* no. 2236.
VALENSI, J. & REBONT, J. 1969 *Agard C.P.* no. 48.
WOOD, C. J. 1964 *J. Roy. Aero. Soc.* **68**, 477–482.